IEEE Access
Multidisciplinary : Rapid Review : Open Access Journal

Received June 27, 2019, accepted July 5, 2019, date of publication July 17, 2019, date of current version August 29, 2019.

Digital Object Identifier 10.1109/ACCESS.2019.2929562

Design, Analysis and Testing of a Component Head Injury Criterion Tester for Pilot

NANNAN CHENG[1], LIANG WANG[1], YONGGUANG LIU[1], AND CHUNYOU ZHANG[1,2]
[1]School of Automation Science and Electrical Engineering, Beihang University, Beijing 100191, China
[2]College of Mechanical Engineering, National University of Inner Mongol, Tongliao 028000, China

Corresponding author: Yongguang Liu (lyg@buaa.edu.cn)

ABSTRACT In a large braking environment, the head of the pilot would collide with the head up display (HUD) because of the aircraft pilot's body leaning forward under inertia. And the preload of the HUD determines whether the head is injured during the collision. Therefore, it is necessary to design a test component for investigating the influence of the mounting preload on head injury during the collision. Consideration of pilot safety, in this paper, the motion characteristics of the pilot is analyzed, and a component of head injury criteria tester for head impact test is established. Given the short-time and high-speed characteristics of the head impact, the driving method adopted hydraulic ejection. This method effectively solves the problems of space limitation and non-reusability in traditional methods. The computational fluid dynamics model and kinematic model of human body are used in this study to simulate the acceleration process. The AMESIM simulation model is set up to study the influence of key parameters on the velocity, angle and acceleration of the system collision moment, to optimize the system parameters and to be verified through experimental studies. The ultimate objective is to achieve that the linear velocity is 11 m/s when the test component rotates at a specified angle. This research can be referred to in the design of a component HIC tester and the study on optimization of fluid flow dynamic characteristics.

INDEX TERMS Preload of the HUD, head injury criteria tester, head impact test, hydraulic ejection, optimize parameters.

I. INTRODUCTION

At present, the research method on head impact test mainly involves driving a Hybrid III50th dummy having an approximate human size and skin structure to collide with a test piece installed at a specified position. By analyzing the parameters such as force, speed and acceleration of the head, it can be used to assess whether the test causes head injury according to the HIC standard [1]–[5]. Hybrid III50th dummy is currently used in collision experiments [6]. The dummy is designed according to the size characteristics of the European and American human body. Hybrid III is a mixed type III dummy whose size meets the 50th percentile adult size of the United States. Its body weight and main size are equivalent to the 95th percentile adult size in our country, which is quite different from the 50th percentile adult size. Besides, the whole body is made of ethylene rubber material to simulate human skin, and the price is very expensive. In local collision of the human body, dummy usually has redundant parts that are not used. It results in great waste [7]. Therefore, it is necessary to simplify the human body structure.

Currently, sled test and ejection test are conducted in the head collision experiment [8]–[11], [18]. Among them, sled test has great requirements on space. The dummy needs to be accelerated over a long distance, so the test conditions have limitations [9], [10]. Ejection test employed pneumatic propulsion system to propel the dummy in order to achieve similar kinematics [9], [10]. However, it's short-time and high-speed characteristics mean that the system is susceptible to interference, such as pressure pulsation. The focus of this paper is to ensure the impact speed while suppressing interference and reducing the speed of the actuator.

In summary, the main research content of this paper is to analyze the pilot's motion characteristics in the braking state, design the structure of the component HIC tester and establish kinematic model based on AMESIM [12]–[15]. On the basis of the mathematical model, carry out parametric modeling and optimization analysis of the ejection lever

The associate editor coordinating the review of this manuscript and approving it for publication was Zheng Chen.

drive mechanism. It provides a reference for the design of the ejection lever drive mechanism. In addition, mathematical modeling of hydraulic circuit was established. The influence of pressure pulsation, accumulator pressure and volume on the velocity and acceleration of the test component is analyzed by AMESIM simulation [15], [16]. Finally, the results are evaluated. The article gives the structural design method of the head test component, which makes the head crash test method more standardized and more scientific, and provides a high reference for the study of the controllability and reliability of the crash test.

II. METHODS

A. HEAD COMPONENT MODEL

When a high-speed aircraft has a sudden braking, it can be equivalent to that the pilot is subjected to a positive acceleration. Ignoring the body's own mitigation effect, the values of the positive and brake accelerations are approximately equal. The movement of the human body being equivalent to rigid body can be regarded as a rotational movement with the lower part of the waist (close to the end of the spine) as the axis of rotation [17]–[19]. Assume that the pilot's lower limbs are fixed, and there is no relative sliding with the seat during braking. An ellipsoid is used to replace the entire hip and lower limb part of the real person. The end of the spine is seen as a rigid connection node between the upper torso and the lower torso. Figure 1 shows the sitting posture model of man model.

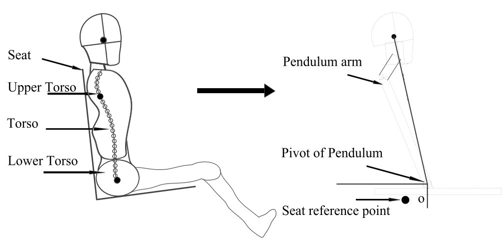

(a) Human sitting posture model **(b) Head component model**

FIGURE 1. Sitting posture model of Man Model.

Head component model is similar to the inverted pendulum structure, in which the pendulum arm is a rigid rod body representing the spine and the upper body torso. The pendulum pivot is located at the lower limb node. Seat reference point refers to the point formed by the intersection of planes drawn from the seat back and the seat pan. The relative position between pendulum pivot and seat reference point should be consistent with the relative position of human lower torso and seat. The model reduces experimental materials and eliminates unnecessary waste caused by use of the 50th percentile Hybrid III dummy. Its highly integrated configuration reduces the area covered of test components. Besides rigid body architecture makes the head component more controllable and repeatable. Moreover, from the ergonomics, the height and weight of a person are directly related to the position of gravity of each part of the human body, the moment of inertia, and the radius of rotation. Too many deviations in the size of the body will cause the test data to deviate from the correct value of the corresponding percentile. In order to simulate the collision process more accurately, the design dimensions of the dummy model refer to the human data and driving environment of Asian pilots. The design dimensions of the dummy model were finally obtained as shown in figure 2 [20]. The dimensions are listed in table 1.

TABLE 1. Relevant parameters of head component.

Symbol	Quantity	Setting value	Measurement
H_1	eye height	706.1	mm
H_2	head height	820.8	mm
S_1	initial horizontal distance between eye and axis	108.8	mm
S_2	ending horizontal distance between eye and axis	375	mm
β_1	initial angle from pendulum arm to vertical direction	6	°
β_2	angle of head impact	22	°

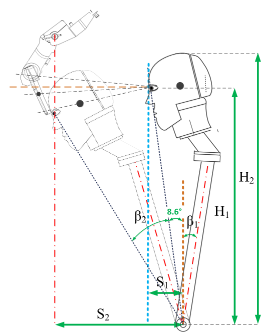

FIGURE 2. Dimensions of head component model.

B. DRIVING METHOD

Pilot's head would collide with the HUD in an emergency braking as a result of expected inertial forces. According to the provisions of the "China Civil Aviation Regulations", the forward longitudinal velocity fluctuation is not less than 10.7 m/s in the case of emergency braking. Accordingly, the initial velocity at the time of impact between the pilot's head and the HUD is 10 ∼ 11m/s. Hydraulic ejection is used for head impact test. Hydraulic ejection is used as the driving method of the system. Compared with pneumatic ejection, hydraulic drive has the advantages of high frequency response, wide speed range, safety and reliability. Moreover, pneumatic ejection requires air compressor, which will occupy more space and generate huge noise.

The 22° rotation angle and a speed of 11 m/s require high performance of the hydraulic cylinder, which adds to the cost of the experiment. The system adopts a two-bar mechanism. And it is hinged with the hydraulic cylinder. During the process of propulsion, the angle between hydraulic cylinder and two-bar mechanism decreases from 180 degrees. Based on the character of triangle, stroke of two-bar mechanism is less than that of traditional mechanism. Therefore, it can greatly reduce the stroke and speed of the hydraulic cylinder. The effect diagram of the system with or without two-bar mechanism or not is shown in Figure 3.

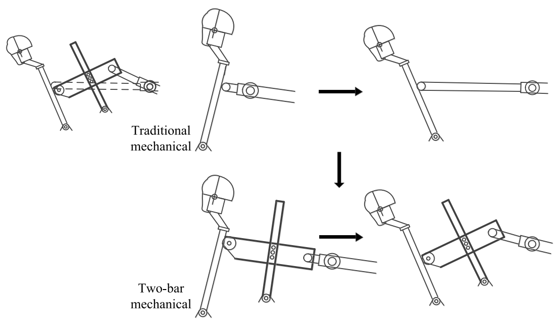

FIGURE 3. Effect diagram of two-bar mechanism.

The hydraulic circuit employs a small displacement oil pump and a large-capacity accumulator. And the small displacement pump can continuously supply oil to the accumulator 1. When the pressure of port A reaches the specified value, the pilot valve of cartridge valve 2 is controlled to make the cartridge valve 2 open. Meanwhile the accumulator 1 can instantaneously release high-flow hydraulic oil and push the piston of hydraulic cylinder to produce high acceleration and speed in a very short time. The accumulator 2 is used to buffer the pressure pulsation caused by the hydraulic pump. Besides, the cartridge valve 1 is a relief valve whose primary function is to ensure that the system works at the specified pressure. When the pressure is higher than the specified pressure, overflow should occur. The hydraulic principle is shown in Figure 4.

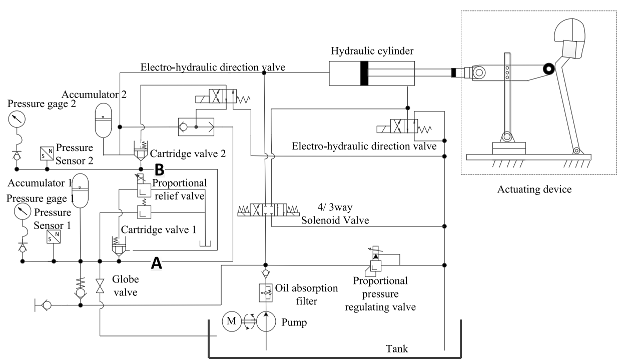

FIGURE 4. Principle diagram of hydraulic system.

C. ANALYSIS OF MOTION CHARACTERISTICS

The hydraulic cylinder drives the two-bar mechanism to rotate so that mechanism applies a thrust to the head test component. And the direction of the initial force is perpendicular to the pendulum arm. In rotating motion, as long as the center and radius of rotation are determined, the angular and linear velocities will not change in virtue of different coordinate systems. As is shown in figure 5, establish rectangular coordinate system, which take the rotation center of the head component as the origin, the pendulum rod as the ordinate, and its vertical direction as the abscissa. In this coordinate system, the initial position of the push rod in the two-bar linkage is in a straight line with the hydraulic cylinder. And the push rod is perpendicular to the rocker of the head test component and the two rods intersects at the point p_0. At t-moment, as shown schematically in Figure 5 when the extension length of hydraulic rod changes Δs, push rod and the rocker intersects at the point $p_n(xy)$.

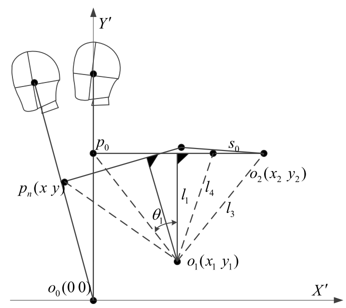

FIGURE 5. Construction design of two-bar mechanism.

According to our above analysis, the mathematical model of the Motion characteristics can be obtained as:

$$\begin{cases} x = -\sin(\theta_1+\theta)\cdot\sqrt{x_1^2+l_1^2}+x_1 \\ y = \cos(\theta_1+\theta)\cdot\sqrt{x_1^2+l_1^2}+y_1 \\ \theta = arc\cos\dfrac{l_3^2+l_4^2-(\Delta s+s_0)^2}{2\cdot l_3\cdot l_4} - arc\cos\dfrac{l_3^2+l_4^2-s_0^2}{2\cdot l_3\cdot l_4} \\ \alpha = \arctan\dfrac{x}{y} \\ \omega = \dfrac{d\alpha}{dt} \\ v = r\cdot\omega \end{cases} \tag{1}$$

where l_1, l_3, $o_1(x_1y_1)$, $o_2(x_2y_2)$, s_0, Δs stand for height of push rod, length of the line o_1o_2, axis of two-bar mechanism, pivot of hydraulic cylinder, initial length of hydraulic cylinder, variation of piston rod length, respectively. Besides, l_4 is the length of the connection between the end of piston rod and o_1-point at the initial time;θ, α, ω, v stand for rotation angle of the two-bar mechanism angle, head impact angle, head impact angular velocity, head impact linear velocity.

In order to study the influence of the structure parameters on head impact angel and linear velocity, the model simulations were performed by using the AMESIM. The simulation results of head component were shown in Figure 6, Figure 7, and Figure 8.

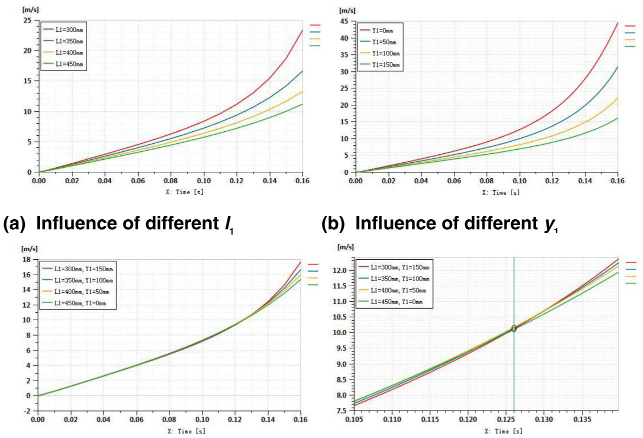

(a) Influence of different l_1 (b) Influence of different y_1

(c) Influence of different $l_1 + y_1$ (d) Local enlargement of figure c.

FIGURE 6. Influence of two-bar mechanism vertical height on speed head impact velocity.

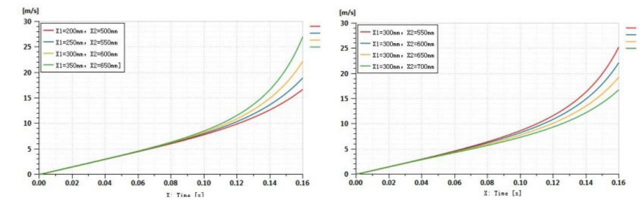

(a) Influence of different x_1 (b) Influence of different x_2

FIGURE 7. Influence of two-bar mechanism transverse length on speed head impact velocity.

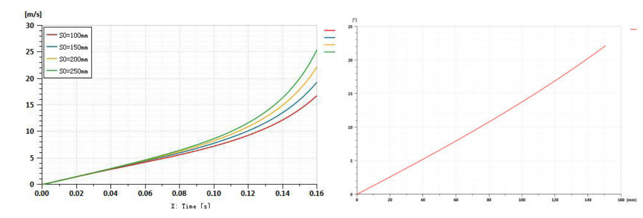

(a) Influence of different s_0 (b) Impact angle of different $\triangle s$

FIGURE 8. Influence of hydraulic cylinder length and variation on head impact characters.

From Figure 6, Figure 7, and Figure 8, we can see that:

(1) Figure 6 (a) and (b) show the comparison curves of impact velocity. It shows that the height of l_1 and y_1 clearly influences head impact velocity. Along with the decreasing of l_1, the impact velocity is getting faster and faster. As the same with l_1, the velocity becomes faster with the decrease of y_1.

(2) Figure 6 (c) shows that the different parameter of l_1+y_1 influences the impact velocity. Holding variable of l_1+y_1 constant, when l_1 increases, the velocity decreases, and system response time improves. Therefore, compared with y_1, l_1 has a greater effect on impact velocity.

(3) Figure 7 shows the influence of x_1 and x_2 on the impact velocity through the comparison curves. Remaining variable of x_2-x_1 constant, when x_1 increases, the velocity increases. Conversely, when x_2 increases, the velocity decreases.

(4) Figure 8 shows the length and stroke of hydraulic cylinder influence on the velocity and angle respectively. With other parameters constant, when s_0 increases, the velocity increases. And the stroke of the hydraulic cylinder determines the head impact angle. When $x_1 = 320$, $x_2 = 583$, $y_1 = 100$, $y_2 = 450$, $s_0 = 200$, the curves of impact angle influenced by stroke of the hydraulic cylinder is showed as Figure 8 (b). Where Δs is 150 *mm*, the head impact angle is 22°. Therefore, the optimal structural parameters are as follows: $x_1 = 320$, $x_2 = 583$, $y_1 = 100$, $y_2 = 450$, $s_0 = 200$, $\Delta s = 150$.

III. MATHEMATICAL MODEL OF HYDRAULIC CIRCUIT

In order to simulate the collision process between the pilot's head and HUD, the hydraulic ejection device is required to provide instantaneous high acceleration for the head test component. After short-term acceleration, centroid speed of the head test component requires to reach 11 m/s. When l_1, $o_1(x_1 y_1)$, $o_2(x_2\ y_2)$ are determined, the value of v entirely depends on the speed of the piston rod of the hydraulic cylinder. The corresponding mathematical model is established according to the hydraulic schematic diagram.

A. HYDRAULIC CYLINDER

Hydraulic cylinder, as the actuator of hydraulic system, realizes energy conversion by the differential pressure between two chambers: converting hydraulic energy into mechanical energy. Single-acting cylinder is employed in the system. The flow of rod less cavity can be represented in a continuous equation.

$$Q = \frac{\pi D^2}{4} v_0 \tag{2}$$

where Q is flow of rod less cavity, D is piston diameter, v_0 is the speed of cylinder rod.

B. CARTRIDGE VALVE

The cartridge valve is a hydraulic control component with two-way unidirectional components as the main body and pilot control and cartridge connection. The cartridge valve has the advantages of small quality, short stroke, quick action, sensitive response, compact structure, good manufacturability, reliable operation, long service life, easy to realize tubeless connection and integrated control, and is especially suitable for high pressure and large flow system. Figure 9 is the equivalent diagram of cartridge valve.

The pressure-flow equation of the pilot solenoid valve can be obtained as:

$$Q_D = C_D A_D \sqrt{\frac{2}{\rho} |P_C - P_D|} \tag{3}$$

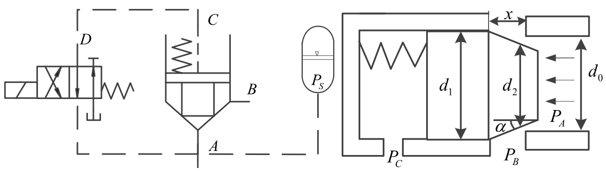

FIGURE 9. Equivalent diagram of cartridge valve.

where Q_D, P_D are orifice flow and pressure of pilot solenoid valve, C_D is the flow coefficient, A_D is the overflow area, and P_C is pressure of the control C-chamber.

The flow continuity equation of the pilot solenoid valve is as follows:

$$Q_C = Q_D + V_D \dot{P}_D / \beta_e \tag{4}$$

where Q_C is flow of control chamber of pilot solenoid valve, V_D is the D-chamber volume of pilot solenoid valve, β_e is oil modulus of volume elasticity.

When the opening pressure is satisfied, the fluid flows unidirectionally, and the spool moves under the action of the fluid pressure, while the movement of the spool affects the fluid flow in turn. Therefore, the motion of the valve and the pressure acting on the disc are coupled with each other. Its mathematical model is very complex. Its complete mathematical model includes at least two differential equations, one for describing liquid flow and the other for describing the motion of the valve core. The differential equation of the motion of the spool is as follows:

$$m_{\mathrm{eq}} \ddot{x} + c_{\mathrm{eq}} \dot{x} = F_{\mathrm{eq}} \tag{5}$$

where m_{eq} and x are the mass and displacement of the valve core respectively, c_{eq} is the equivalent impedance of valve core motion, F_{eq} is the force acting on the valve core.

$$F_{\mathrm{eq}} = F_{\mathrm{g}} - F_{\mathrm{d}} \tag{6}$$

where F_{g} is fluid force, F_{d} is spring function force.

$$F_{\mathrm{d}} = k_1(x + x_0) \tag{7}$$

where k_1 is spring elastic stiffness coefficient, x_0 is spring pre-compression.

$$\begin{cases} F_{\mathrm{g}} = A_x \cdot P_A + (A - A_x) \cdot P_B - P_C \cdot A \\ A_x = \frac{\pi}{4} d_2^2 = \frac{\pi}{4}(d_0 - 2x \sin\alpha \cos\alpha)^2 \\ A = \frac{\pi}{4} d_1^2 \end{cases} \tag{8}$$

where A_x, P_A are area and pressure of oil inlet A-chamber respectively when spool opening was x, A and P_C are area and pressure of the control C-chamber respectively, P_B is pressure of oil outlet B-chamber.

The pressure-flow equation of cartridge valve orifice is

$$Q_A = c_q \cdot \pi x \cdot \sin\alpha (d_0 - x \cdot \sin\alpha \cdot \cos\alpha) \cdot \sqrt{\frac{2\,|P_A - P_B|}{\rho}} \tag{9}$$

where ρ is fluid density, c_q is flow coefficient.

The flow continuity equation of cartridge valve control chamber is:

$$Q_C = A\dot{x} - V_C \dot{P}_C / \beta_e \tag{10}$$

where V_C is volume of control chamber, c_q is flow coefficient.

The pressure-flow equation of cartridge valve control chamber is:

$$Q_C = c_L A_L \operatorname{sgn}(P_C - P_D) \sqrt{\frac{2\,|P_C - P_D|}{\rho}} \tag{11}$$

where c_L is the flow coefficient and A_L is the cross section area of the pipeline.

The equation of equivalent chamber flow-pressure for pipeline volume effect is as follows:

$$Q_E = c_E A_E \operatorname{sgn}(p_E - p_A) \cdot \sqrt{\frac{2\,|P_A - P_E|}{\rho}} \tag{12}$$

where c_E is the flow coefficient, A_E is the entrance area of equivalent cavity respectively, and P_E is the pressure of equivalent cavity.

The model of equivalent chamber for pipeline volume is as follows:

$$\frac{\rho L}{A_L} \dot{Q}_E = p_S - p_E \tag{13}$$

where L is the length of pipeline and p_s is oil source pressure.

The flow continuity equation of cartridge valve inlet is:

$$Q_E = Q_A + V_A \dot{P}_A / \beta_e \tag{14}$$

where V_A is the equivalent volume of cartridge valve inlet.

The flow continuity equation of cartridge valve outlet is:

$$Q_A = Q_L + V_B \dot{P}_B / \beta_e \tag{15}$$

where Q_L is the pipeline flow, V_B is the equivalent volume of cartridge valve outlet.

$$Q_L = c_L A_L \sqrt{\frac{2P_B}{\rho}} \tag{16}$$

IV. EXPERIMENT AND SIMULATION

A. EFFECT OF PRESSURE FLUCTUATION ON DYNAMIC BEHAVIOR OF VALVE CORE

According to the above formulas, the dynamic and steady-state process of the spool are affected by working pressure of the system and pipe length which in turn affects the acceleration and velocity of the head test component. Based on the principle and mathematical model of cartridge valve, AMESIM is used for modeling and simulation as Figure 10. And the nominal values of main parameters of the cartridge valve loop are listed in table 2. Considering that in the working process, because of the gear pump pressure pulsation, it is necessary to research the impact of pressure pulsation on the dynamic and steady-state process of the valve core. The less teeth of external meshing gear pump, the larger the pulsation

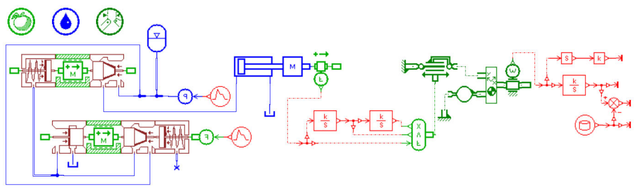

FIGURE 10. AMESIM model.

TABLE 2. Nominal value of main parameters of cartridge value loop.

Symbol	Quantity	Setting value	Measurement
α	valve core angle	15	°
A	area of C port	804	mm^2
x_0	spring compression length	18	mm
m	mass of core valve	1.1	kg
k_1	spring elastic stiffness coefficient	1.2×10^5	N/m
V_D	pilot volume	14300	mm^3

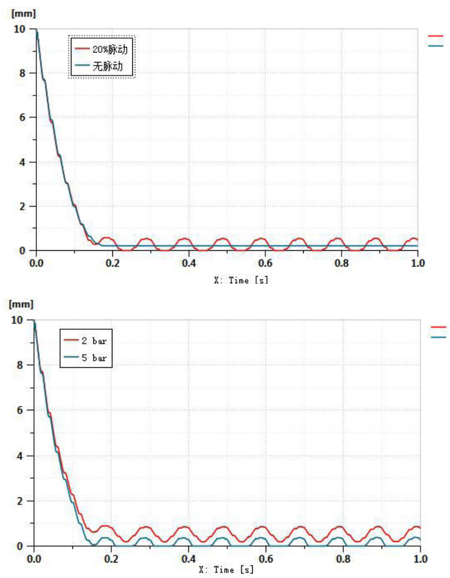

FIGURE 11. Influence of pressure fluctuation on the displacement.

rate will be. And the highest pulsation rate can be more than 0.2. Therefore, we chose 0.2 as the pulsation rate in this paper.

The working pressure sets 3 *bar* and pressure fluctuation is 20%. Under the same conditions that other parameters are the same, the dynamic response of cartridge valve core is simulated under pressure fluctuation and no pressure fluctuation. The result of simulation is as Figure 11. The dynamic response process of cartridge valve core under these two conditions is observed as shown in the figure. It can be seen that the displacement of the spool oscillates periodically because of the pressure fluctuation. Figure 11 also shows the effect of 20% pressure fluctuation on the displacement of the valve core when the system operates at 3 bar and 8 bar respectively. A conclusion can be drawn that the greater the system working pressure, the less the impact of pressure fluctuation. Moreover, the opening and pressure of cartridge valve determine the flow of the hydraulic cylinder, and then affect the piston rod speed. In order to reduce the velocity instability caused by pressure fluctuation, it is necessary to select an appropriate accumulator to suppress the oil source fluctuation.

B. EFFECT OF ACCUMULATOR PRESSURE AND VOLUME ON DYNAMIC BEHAVIOR OF HIC TESTER

Combining with the principle and mathematical model of cartridge valve, the influence of accumulator pressure and volume on acceleration, velocity and angle of head test component is studied by AMESIM simulation. When other parameters are the same, the system pressures are 10 *bar*, 20 *bar*, 30 *bar* and 40 *bar* respectively, observing the curve of acceleration, centroid velocity and angle under different pressure as Figure 12. The same method is used for study on volume and volumes are $0.63L$, $1L$, $1.6L$, $2.5L$ respectively. The simulation result is as Figure 13. Overshot at 0.06s, the piston rod of the hydraulic cylinder extends to the limit position and its acceleration and velocity suddenly change to 0. In fact, head component model maintaining the pre-mutation velocity collides with the HUD.

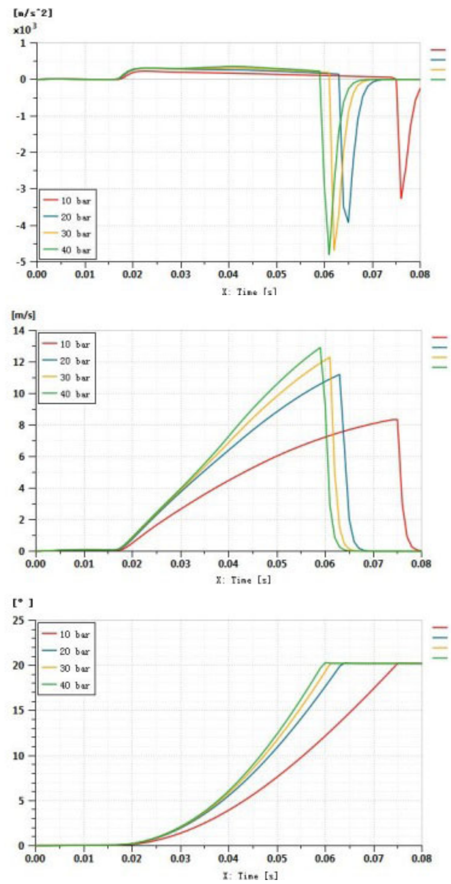

FIGURE 12. Influence of pressure on the acceleration, velocity and angle.

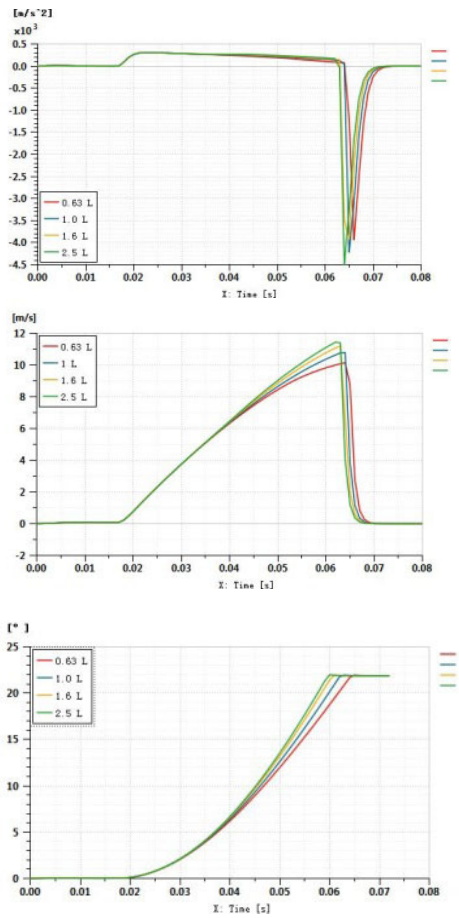

FIGURE 13. Influence of volume on the acceleration, velocity and angle.

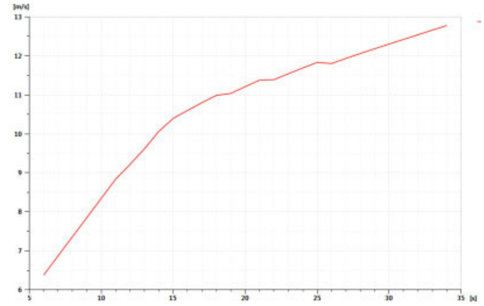

FIGURE 14. The relationship between pressure and velocity.

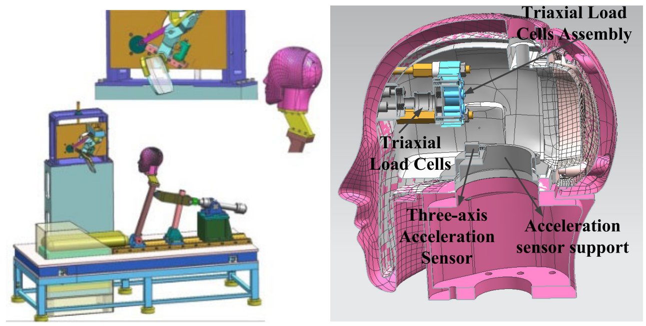

(a) 3D structure (b) 3D model of head

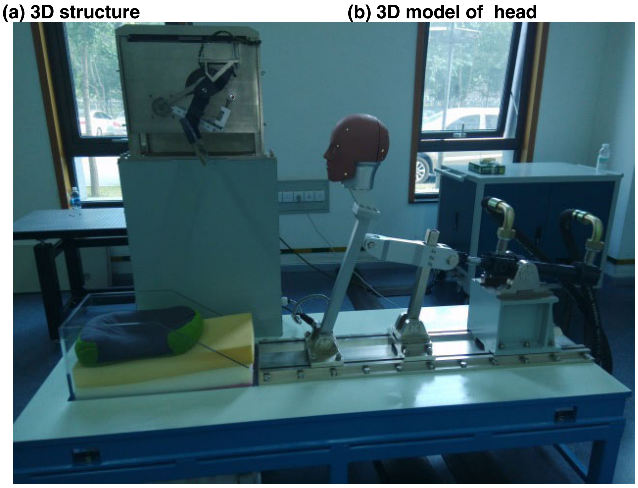

(c) Experimental apparatus

FIGURE 15. Structure of HIC Tester.

The simulation results show that along with that the increase of accumulator pressure, the acceleration increases at the moment of loading. Moreover, the accumulator pressure directly affects the final velocity of the head impact. The pressure of accumulator increases, the acceleration and velocity of the test component increase when it reaches the specified position. Figure 13 show that the larger the accumulator's volume, the greater the velocity and acceleration of the test component. Compared with accumulator pressure, volume has less influence on velocity and acceleration. Therefore, choosing the appropriate accumulator pressure and volume can achieve the purpose of adjusting the end velocity of the head component. At the moment of 0.06s, the extension of the piston rod of the hydraulic cylinder to its limit position causes the acceleration and speed of two-bar mechanism drop sharply to 0. Meanwhile, the head component is separated from the two-bar mechanism, and maintains the speed before separation to collide with the HUD. When accumulator volume is 1.6L, the relationship between pressure and velocity is shown in Figure 14.

C. EXPERIMENTAL VERIFICATION

Generally speaking, the head impact component for simulating pilots mainly includes the dummy head and spine, drive device and hydraulic cylinder actuator. The base of each part is installed on the linear guide rail, the whole device is loaded by the isolation platform and the buffer device is designed in the position of the dummy head falling forward. In addition, three-axis acceleration sensor and triaxial load cell which are mounted in the head are used to measure the acceleration and force at the time of collision respectively. An encoder designed at the rotation axis of the head test component is used to measure its rotation angle and then obtain the linear velocity of the head center of mass. The total length of the test bed is 2060 mm, the height is 1780 mm, and the weight is 1120 kg.

As shown in Figure 15, firstly start the motor; when the pressure reaches 20bar, open the cartridge valve 2; then the

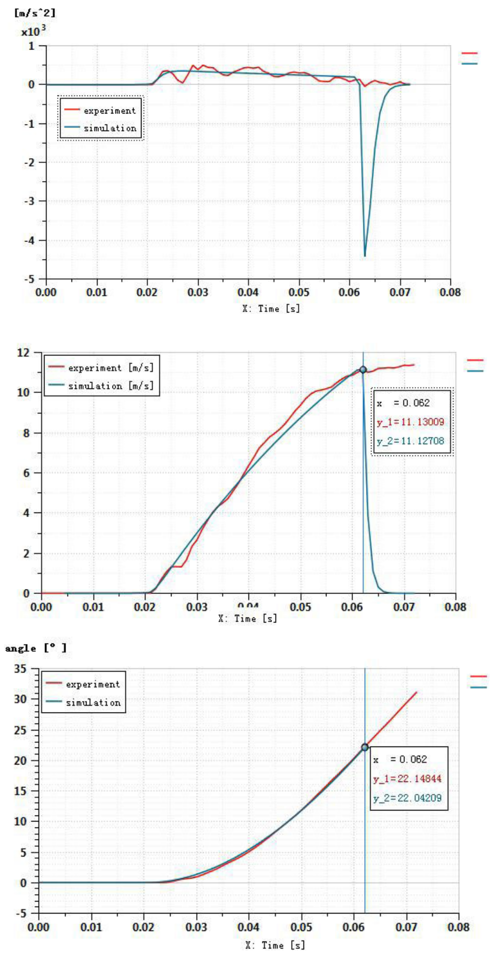

FIGURE 16. Comparison of simulation and experiment results.

piston rod of the hydraulic cylinder drives the head test component to rotate through the two-bar mechanism. In summary, the final structural parameters are set as $x_1 = 0.32$, $x_2 = 0.583$, $y_1 = 0.1$, $y_2 = 0.45$, $s_0 = 0.2$, the system pressure is 20 bar, and the volume of accumulator is 1.6L. The simulation results are compared with the experiments. The structure of the HIC tester is shown in Figure 15 and the comparison of simulation and experiment results are shown in Figure 16. The result shows the simulated and measured resulted such as the acceleration, velocity and angel are in good agreement with each other. Experiments verify the correctness of the mathematical model. Overshot at 0.062s, the piston rod of the hydraulic cylinder extends to the limit position and its acceleration and velocity suddenly change to 0.

V. CONCLUSION

To build a foundation for the optimization of HIC tester, the spool of cartridge valve dynamic characteristics are analyzed by building a mathematical model and setting up an experimental station. In addition, the influences of key system parameters are researched. Conclusions can be drawn as follows:

(1) The experimental results are consistent with the simulation ones, and the proposed mathematical model is demonstrated to be effective.
(2) Increasing the horizontal length of 2-bar mechanism can enlarge the speed of hydraulic cylinder, and decreasing the height of 2-bar mechanism also can enlarge the speed of hydraulic cylinder.
(3) Increasing the stroke of hydraulic cylinder, the angel of head impact increases and the slope of curve increases.
(4) When the pressure is relatively low, the displacement of the spool is susceptible to the pressure fluctuation and produces periodic oscillation. To avoid the periodic oscillation, the pressure of accumulator can be selected higher within defined limits.
(5) Increasing the pressure and volume of accumulator, the acceleration and velocity of the test component increase when it reaches the specified position.

This research provides a basis for the design and performance optimization of HIC tester component. The HIC tester component provides experimental evidence for installation and debugging of HUD.

REFERENCES

[1] L. W. Schneider, W. H. Hardy, A. I. King, S. W. Rouhana, M. S. Beebe, M. J. Salloum, R. H. Eppinger, and M. P. Haffner, "Development of an advanced ATD thorax system for improved injury assessment in frontal crash environments," SAE, Warrendale, PA, USA, Tech. Rep. 922550, 2015.
[2] J. K. Foster, G. J. O. Kort, and M. J. Wolanin, "Hybrid III-A biomechanically-based crash test dummy," SAE, Warrendale, PA, USA, Tech. Rep. 770938, 1977.
[3] J. Versace, "A Review of the Severity Index," SAE, Warrendale, PA, USA, Tech. Rep. 710881, 971, pp. 771–796.
[4] E. S. Gurdjian, H. R. Lissner, F. R. Latimer, B. F. Haddad, and J. E. Webster, "Quantitative determination of acceleration and intracranial pressure in experimental head injury: Preliminary report," *Neurology*, vol. 3, p. 417, Jun. 1953.
[5] E. S. Gurdjian, V. L. Roberts, and L. M. Thomas, "Tolerance curves of acceleration and intracranial pressure and protective index in experimental head injury," *J. Trauma Acute Care Surg.*, vol. 6, pp. 600–604, Sep. 1966.
[6] G. W. Wood, M. B. Panzer, C. R. Bass, and B. S. Myers, "Viscoelastic properties of hybrid III head skin," *Int. J. Mater. Manuf.*, vol. 3, pp. 186–193, Jan. 2010.
[7] H. Huimin, L. Xianxue, D. Li, and Z. Zhaoyi, "A summary of the research on automobile collision dummy," *Standard Sci.*, vol. 7, pp. 6–9, Apr. 2015.
[8] H. Nagarajan, M. McCoy, C. S. Koshy, and H. M. Lankarani, "Design, fabrication and testing of a component HIC tester for aircraft applications," *Int. J. Crashworthiness*, vol. 10, pp. 515–523, Mar. 2005.
[9] R. DeWeese, D. Moorcroft, C. K. Thorbole, and H. M. Lankarani, "Use of a head component tester to evaluate the injury potential of an aircraft head-up display," *Int. J. Crashworthiness*, vol. 16, pp. 385–395, Aug. 2011.
[10] C. K. Thorbole, and H. M. Lankarani, "Performance evaluation of HIC component testing device with a flexible neck using computational model," *Int. Mech. Eng. Congr. Expo.*, vol. 1, pp. 423–429, Jan. 2008.
[11] H. M. Lankarani, C. S. Koshy, and C. K. Thorbole, "Design and validation of a component Head Injury Criteria tester for aerospace applications," in *Proc. 5th Int. Design Eng. Tech. Conf. Comput. Inf. Eng. Conf.*, Jan. 2005, pp. 329–337.
[12] X. Gao and Y. Liu, "Research of giant magnetostrictive actuator's nonlinear dynamic behaviours," *Nonlinear Dyn.*, vol. 92, no. 3, pp. 793–802, May 2018.
[13] Y. Liu, X. Gao, and Z. Pei, "Research of impact load in large electrohydraulic load simulator," *Math. Problems Eng.*, vol. 7, Jul. 2014, Art. no. 821419.

[14] Y. Liu, X. Gao, and X. Yang, "Research of control strategy in the large electric cylinder position servo system," *Math. Problems Eng.*, vol. 7, Jan. 2015, Art. no. 167628.
[15] Y. Shi, B. Zhang, M. Cai, and X. D. Zhang, "Numerical simulation of volume-controlled mechanical ventilated respiratory system with 2 different lungs," *Int. J. Numer. Methods Biomed. Eng.*, vol. 33, Sep. 2017, Art. no. e2852.
[16] X. Gao, Y. Liu, H. Guo, and X. Yang, "Structural design of giant magnetostrictive actuator," *AIP Adv.*, vol. 8, no. 6, 2018, Art. no. 065211.
[17] B. Tolea, A. I. Radu, H. Beles, and C. Antonya, "Influence of the geometric parameters of the vehicle frontal profile on the pedestrian's head accelerations in case of accidents," *Int. J. Automot. Technol.*, vol. 19, no. 1, pp. 85–98, Feb. 2018.
[18] M. Hitosugi, T. Koseki, Y. Kinugasa, T. Hariya, G. Maeda, and Y. Motozawa, "Seatbelt paths of the pregnant women sitting in the rear seat of a motor vehicle," *Chin. J. Traumatology*, vol. 20, no. 6, pp. 343–346, Dec. 2017.
[19] M. Hitosugi, T. Koseki, T. Hariya, G. Maeda, S. Moriguchi, and S. Hiraizumi, "Shorter pregnant women restrained in the rear seat of a car are at risk for serious neck injuries: Biomechanical analysis using a pregnant crash test dummy," *Forensic Sci. Int.*, vol. 291, pp. 133–137, Oct. 2018.
[20] X. W. Wang, X. G. Yuan, M. Z. Sun, R. D. Wang, and F. M. Peng, "Changing tendency of dimensions of mixed type airplane pilots and its human engineering significance," *Beijing Univ. Aeronaut. Astronaut., J.*, vol. 26, no. 5, pp. 547–551, Oct. 2000.

NANNAN CHENG was born in Anhui province, China, in 1990. She received the bachelor's degree in Beijing Information Science and Technology University, and the master's degree from Beihang University.

She is currently pursuing the Doctoral degree in automatical science and electrical engineering from Beihang University, in 2016. Her major is mechanical electronics. Her research interests include hydraulic servo control, smart material and structure, and nonlinear active vibration control.

LIANG WANG was born in 1962. In 1985, he graduated from Harbin institute of Marine engineering. In 1988, he received the M.S. degree in fluid transmission and control specialty from Harbin Institute of Technology, and the Ph.D. degree from Beihang University, in 2000, where he did the Postdoctoral Research, from 2000 to 2002.

Since 2002, he taught in the Department of Mechanical and Electronic Engineering of Beihang Automation College. He is a Professor of mechanical and electronic engineering and Ph.D. supervisor. In 2005, he also serves as the Director of the Engineering Training Center (National demonstration Center) of Beihang University.

YONGGUANG LIU was born in 1967. In 1989, he graduated from Harbin Institute of Technology. In the same year, he was assigned to Harbin Steam Turbine Factory as an Engineer. In 1994, he was admitted to Harbin Institute of Technology as a Graduate Student. In December 1999, he received the Ph.D. degree and also the Postdoctoral Research from Tsinghua University, in 1999–2001.

Since 2002, he has been working with the Department of Mechatronic, Beihang University, as an Associate Professor. His research interests include hydraulic servo control, industrial robots, network control, giant magnetostrictive actuator, and nonlinear active vibration control.

CHUNYOU ZHANG received the B.S. and M.S. degrees in mechanical manufacturing and automation from the Agricultural University of Inner Mongolia, China, in 2000–2008. He is currently pursuing the Doctoral degree with Beihang University, from 2011. Since 2008, he taught in the Department of Mechanical Engineering of National University of The Inner Mongol. He is an Associate Professor, and the Master's Supervisor.